World Academy of Science, Engineering and Technology
International Journal of Structural and Construction Engineering
Vol:16, No:4, 2022

Development of the Maturity Sensor Prototype and Method of Its Placement in the Structure

Ye. B. Utepov, A. S. Tulebekova, A. B. Kazkeyev

***Abstract*—**Maturity sensors are used to determine concrete strength by the non-destructive method. The method of placement of the maturity sensors determines their number required for a certain frame of a monolithic building. This paper proposes a cheap prototype of an embedded wireless sensor for monitoring concrete structures, as well as an alternative strategy for placing sensors based on the transitional boundaries of the temperature distribution of concrete curing, which were determined by building a heat map of the temperature distribution, where unknown values are calculated by the method of inverse distance weighing. The developed prototype can simultaneously measure temperature and relative humidity over a smartphone-controlled time interval. It implements a maturity method to assess the in-situ strength of concrete, which is considered an alternative to the traditional shock impulse and compression testing method used in Kazakhstan. The prototype was tested in laboratory and field conditions. The tests were aimed at studying the effect of internal and external temperature and relative humidity on concrete's strength gain. Based on an experimentally poured concrete slab with randomly integrated maturity sensors, it the transition boundaries form elliptical forms were determined. Temperature distribution over the largest diameter of the ellipses was plotted, resulting in correct and inverted parabolas. As a result, the distance between the closest opposite crossing points of the parabolas is accepted as the maximum permissible step for setting the maturity sensors. The proposed placement strategy can be applied to sensors that measure various continuous phenomena such as relative humidity. Prototype testing has also revealed Bluetooth inconvenience due to weak signal and inability to access multiple prototypes simultaneously. For this reason, further prototype upgrades are planned in the future work.

***Keywords*—**Heat map, placement strategy, temperature and relative humidity, wireless embedded sensor.

I. Introduction

THERE are many methods for determining the compressive strength of concrete. All methods are categorized as destructive and non-destructive [1]. The essence of the destruction method is to test standard specimens in compression on special equipment. In doing so, the specimens are destroyed [2]. The disadvantage of this method is the increased labor intensity of the test, which consists in the preparation of specimens. Specimens can be obtained by cutting a standard size specimen from an existing concrete structure or by sampling commodity mixtures from each batch when concreting monolithic concrete or reinforced concrete structures of a specified project grade and pouring the mixture into the test cube formwork [3]. In the first case, specimens are not always obtained due to the nature of the structure to be tested. In the second case, the specimens may not reflect the actual state of the strength gain due to different curing conditions of the concrete at the site and in the laboratory [4]. Also, due to the high rate of supply of concrete mix to the site, the quality of sampling for testing may decrease. An alternative to the destructive method is the non-destructive method of concrete strength testing. Non-destructive testing is aimed on the study of parameters of the structure without causing damage to the original part of the structure [5]. Non-destructive methods for determining the strength of concrete are based on the bond between the strength of concrete and indirect strength characteristics. The most common method of testing the strength of concrete is the shock impulse method, the essence of which is to record the energy of impact, which occurs at the moment of collision of the striker of a special device with the surface of concrete [6]. The disadvantage of the shock impulse method is the limited working radius of the device - strength can only be determined in the specific test area in a layer up to 50 mm deep, not in the entire structure [7]. Thus, in order to obtain a complete picture of the strength gain it is necessary to perform tests at multiple points of the same element.

The above-mentioned strength control methods have their definite disadvantages in the form of labor intensiveness and relative cost, which can be solved with the help of modern technologies, such as sensors embedded in concrete, machine learning and artificial intelligence [8]-[12]. Through continuous monitoring of the internal condition of the reinforced concrete structure, rapid measurement is achieved, making it possible to dismantle the formwork earlier than expected, saving time and thus financial resources [13]. However, during the analysis of foreign sensors it was found out that the existing analogues due to the high cost of imports and lack of regulation, have not found application on construction sites in Kazakhstan. The peculiarity of the sensors is the preliminary analysis of the temperature regime of concrete curing by conducting a series of laboratory tests of standard concrete specimens [14]. As a result, the efficiency of application of existing foreign analogues of sensors on local construction sites raises certain doubts, because it is almost impossible to pick up the same concrete as on the construction site in a remote laboratory made of completely different inert materials. Adjusting the chemical and particle size distribution of concrete using methods of equivalent materials adds some uncertainty and error to the results of strength determination. Moreover, due to high cost for local consumers (from 30 thousand tenge and more), the use of

Ye. B. Utepov is with the R&D of CSI Research&Lab LLP, Nur-Sultan, 010000 Kazakhstan (corresponding author, phone: +7 (700) 210-17-33; e-mail: utepov-elbek@mail.ru).

A. S. Tulebekova and A. B. Kazkeyev are with the R&D of CSI Research&Lab LLP, Nur-Sultan, 010000 Kazakhstan (e-mail: krasavka5@mail.ru, alizhan7sk@gmail.com).

existing foreign analogues is economically inexpedient. The cost of sensors also comes from the cost of laboratory testing, which is much higher abroad than in local laboratories in Kazakhstan. These inconveniences result in the need for a more effective domestic solution for monitoring reinforced concrete structures, based on a number of parameters that affect the strength gain of freshly paved concrete. However, despite the fact that the use of such innovative methods for determining the strength of concrete is impossible in Kazakhstan due to the lack of relevant normative and technical documents, regulations and standards, we have developed a prototype sensor capable of measuring temperature and humidity when immersed in the body of concrete and transmitting the results wirelessly to a mobile device (smartphone) via Bluetooth. The smartphone, in turn, calculates the strength using known methods.

The study also developed a strategy for placing sensors in the body of the reinforced concrete structure, because previous studies had little coverage of this issue. Accuracy of the received data on durability of a structure depends on placing of sensors in concrete. Insufficient number and incorrect placement of sensors can distort the final result, when too many of them can have a negative impact on saving money.

As already known, concrete curing is an exothermic process [15]. During hydration, the temperature inside the concrete gradually rises and then slightly falls, indicating that the strength gain is complete [16]. Measurement of the internal temperature of the concrete over a certain period of time helps to make decisions about prematurely removing the formwork from the structure, which in turn saves costs and time [17]. It is proved that there is some correlation between temperature and concrete strength, which allows to estimate the actual compressive strength of concrete [16], [18]-[21]. According to [22], temperature is a continuous phenomenon, i.e., its value changes smoothly across the entire surface up to the boundary (hereinafter referred to as the transition boundary), where the influence of other factors prevails. It is assumed that the transitional boundary of temperature distribution takes elliptical forms. Therefore, the largest sensor spacing step should be smaller than the largest diameter of the elliptical form of the temperature transitional boundary. For better visualization, the color heat map of temperature distribution described in [23] can be used.

II. Prototype Development

The essence of the work of the prototype is as follows: before the beginning of pouring the sensor is placed in the concrete body by attaching it to the reinforcement with a clamp. After that the device is started, the interval at which the sensor will measure temperature and humidity in the concrete body is set. The received data are then transmitted to a smartphone using the Bluetooth wireless data transfer protocol. A specially developed mobile smartphone application analyses these data and reports on the actual strength of the concrete. A special feature of the strength control with sensors is the preliminary laboratory analysis. Based on the results of this analysis, a correlation between temperature, humidity and strength is built up, allowing the current strength of the concrete to be determined via the embedded sensor.

The architecture of the prototype is based on the Internet of Things (IoT) concept. IoT architecture includes: on the one hand, a large number of peripherals with low computing power, low power consumption, high speed response to events, and on the other hand, cloud servers with high computing power for processing large volumes of data, their storage and classification, often with elements of machine learning and analysis (Fig. 1).

Fig. 1 Prototype IoT-architecture

The case of a prototype is printed on the 3D-printer from a material acrylonitrile butadiene styrene (ABS-plastic) and has dimensions of 86×86×49 mm. It consists of the lower part and the upper part (cap), which are connected to each other by means of eight bolts. The waterproofing of the connection is ensured by a rubber gasket.

The functionality of the prototype is implemented on the basis of the Arduino Nano 3.0 microcontroller with the possibility of connecting additional modules to it. Application of Arduino as a basis has allowed to simplify and accelerate considerably process of development at the expense of already existing built-in modules, and also special expansion slots which have allowed to connect to the microcontroller the Bluetooth module, and also the temperature sensor with a cable 100 cm. The humidity sensor is built into the housing and is also connected to the microcontroller via an expansion slot. The memory module is built into the microcontroller and is several megabytes long enough to store measurement data for several months. The prototype is powered by three AA batteries. Fig. 2 shows the components of the prototype.

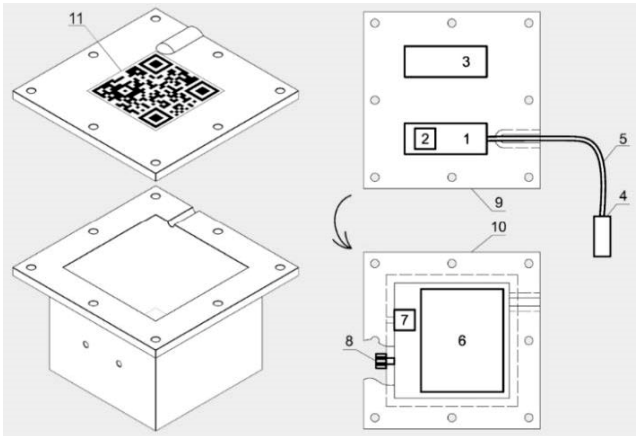

Fig. 2 Prototype components: 1-Microcontroller; 2-Memory; 3-Wireless network module; 4-Temperature sensor; 5-Connecting cable; 6-Power supply; 7-Relative humidity sensor; 8-Switch; 9-Bottom element of the case; 10-Top element of the case; 11-QR identification code

The final development cost of the prototype was 10,200 KZT, which is about $27 (at currency rate of 377 KZT for $1). The cost ratio of the prototype components is presented in Table I.

TABLE I
COST RATIO OF THE PROTOTYPE COMPONENTS

№	Components	Number	Proportion, %
1	Microcontroller Arduino Nano 3.0 with memory	1	24
2	Bluetooth module	1	15
3	Temperature sensor with 100 cm cable	1	12
4	Relative humidity sensor	1	12
5	AA batteries	1	3
6	Switch	1	5
7	Case printed in a 3D printer	1	29
8	QR identification code	1	free

It should be noted that the cost of development does not include labor. The cost of 10200 tenge can be reduced at mass production of industrial models of the sensor.

III. TESTING THE PROTOTYPE

To test the performance of the prototype in the laboratory, 18 cylindrical specimens were made of M350 class B25 concrete. The 15 control specimens were tested in compression according to standard regulations for 1 day, 3 days, 7 days, 14 days and 28 days. Two specimens were used to record the internal temperature of the concrete during curing, and the latter measured the internal humidity. Parallel to the internal parameters, the ambient temperature was also recorded. The measurements were taken over a period of 4 days at 1-hour intervals. This measurement mode was chosen because it is important to know the internal condition of the concrete on the construction site during the first 3-4 days. Further measurements up to 28 days were taken at 6-hour intervals.

According to the results of tests, the 15 control specimens within 7-8 days showed compressive strength of about 30 MPa. On 28 days, the compressive strength was 33.53 MPa, which corresponds to M350 brand and B25 class. Fig. 3 shows the results of testing the compressive strength of 15 specimens.

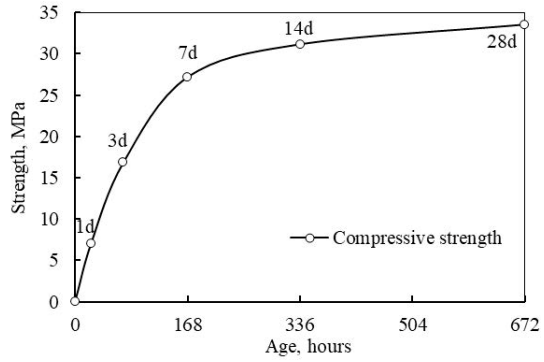

Fig. 3 Compression test results

The results of measurements (Fig. 4) of the internal temperature of the two specimens showed a temperature increase of more than 45 °C during the first 3-4 days with a peak value of 47 °C within a few hours. This temperature increase indicates an active hydration process. Then the temperature decreased to 22 °C and slightly fluctuated with an amplitude of 5 °C until it was equal to the laboratory air temperature, which indicates a slowdown in hydration. The laboratory air temperature during the measurements slightly fluctuated between 8 °C and 10 °C. At the same time, the relative humidity of the environment fluctuated between 54% and 88%. At the moment of temperature rise, a decrease in relative humidity was observed, i.e., an inverse relationship between humidity and temperature was observed. At the beginning of measurements, the humidity level of the last specimen was close to 100%. However, during hydration the humidity decreased. By 28 days, the humidity level was 70%.

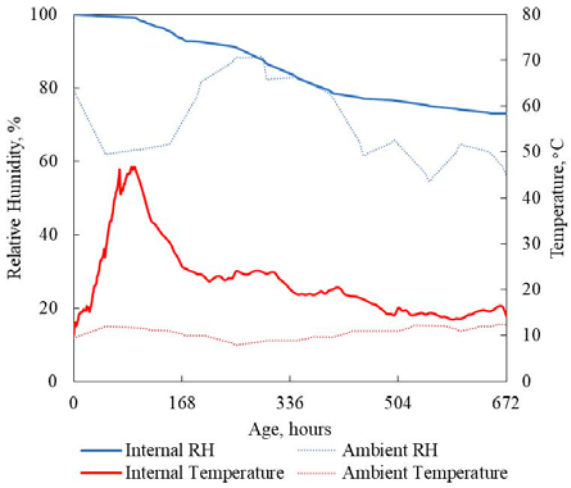

Fig. 4 Recordings of internal and ambient parameters at the laboratory

Using (1), a strength gain was calculated, the data of which would be included in the graph (Fig. 5).

$$M(t) = \sum(T_a - T_0)\Delta t \quad (1)$$

where: $M(t)$ = the temperature-time factor at the age t (degree-hours), Δt = a time interval (days or hours), T_a = average concrete temperature during time interval (Δt·°C), T_0 = datum temperature (taken as -10 °C).

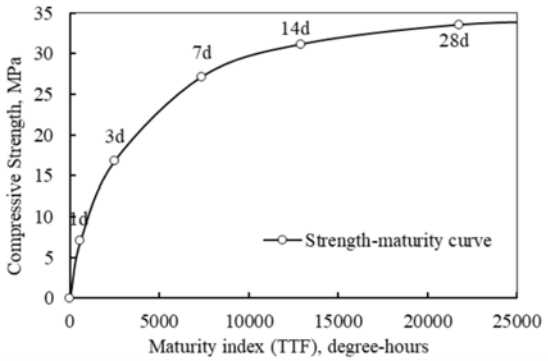

Fig. 5 Strength-maturity relationship of concrete B25 M350

The calculations revealed the concrete strength for 28 days amounted to 21792-degree hours, which corresponds to 33.53 MPa. The obtained strength curve was later used to assess the in-situ strength of concrete at different ages.

In the field, the test was carried out as follows: a 0.4 cubic meter plate with a similar mixture to that of the laboratory test was poured into the center of which a prototype transducer was placed. The time intervals for measuring the humidity and temperature were set in the same way as in a laboratory test. The prototype collected data for up to 28 days. The data obtained were extracted from the prototype via Bluetooth to a smartphone and recorded in Excel. The measurement results are visualized in Fig. 6.

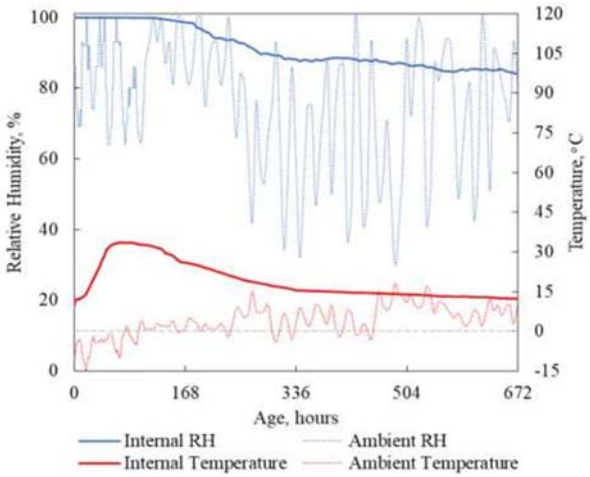

Fig. 6 Recordings of internal and ambient parameters at the field

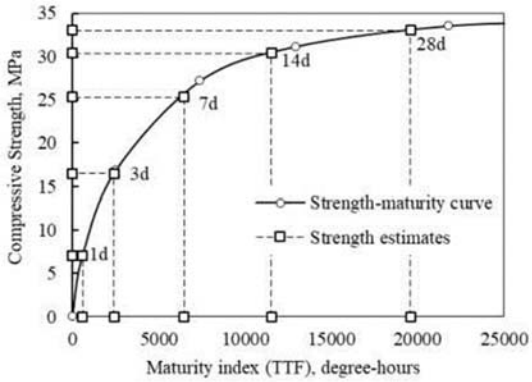

Fig. 7 Estimation of in-place concrete strength

According to the measurements, the ambient temperature from the beginning of measurements ranged from -15 °C to +18 °C. However, in general, the graph of temperature changes shows its growth. It is obvious that large fluctuations in ambient temperature have affected the hydration process, as evidenced by the temperature inside the concrete, -36.6 °C. This temperature is the highest point of the graph and has been gradually decreasing. Relative humidity also showed large fluctuations of 30% to 100%. However, the inverse relationship between temperature and humidity has been preserved. For 5 days, the humidity inside the concrete was close to 100%, and then began to drop to 84% closer to 28 days.

Using (1), a strength gain was calculated, the data of which were included in the existing laboratory test schedule (Fig. 7).

As expected, the concrete's strength gain in the field was lower than expected in the laboratory.

IV. Development of a Sensor Placement Strategy

In order to create a heat map and determine the transitional boundaries of temperature distribution in a 12 x 6 x 0.2 m plate, prototypes of sensors were installed in random positions as shown in Fig. 8.

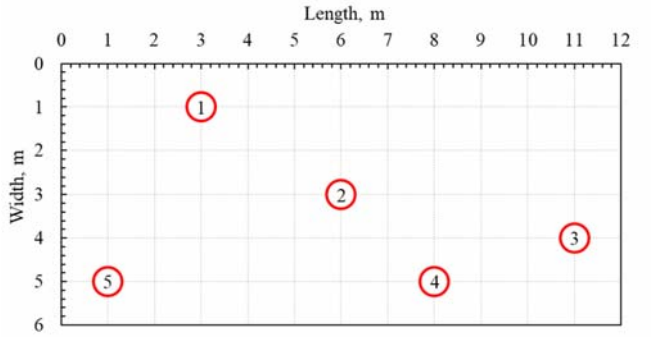

Fig. 8 Locations of the maturity sensors

The slab was filled with a mixture of M350 grade B25. After pouring, the sensors measured the temperature for 28 days. At the same time, the ambient temperature was 10-12 °C and the thermo-physical properties of the formwork were not taken into account, as its influence was considered insignificant.

After the measurements were completed, the data were uploaded to the Excel table on 672 pages, each corresponding to each hour of measurements.

Each sheet was a two-dimensional plane of 1200 x 600 cells, where each cell was equal to 10 x 10 cm plate size. Sensor readings were taken as reference points in the specified places of the plate.

Using the inverse distance weighing (IDW) method, unknown temperature values for other points were determined from already known values. Thus, a (2) was assigned to each cell of the two-dimensional plane in which the weighting factors represented the distances from each cell to the locations of reference points.

$$t_c = \frac{\sum_{i=1}^{n} \frac{t_i}{d_i^p}}{\sum_{i=1}^{n} \frac{1}{d_i^p}} \quad (2)$$

where: t_c = unknown value of temperature in the cell; I = number of reference point; t_i = known value of temperature at the reference point i; d_i = search distance from the cell to the reference point i; p is power of IDW (p = 2) [24].

The heat map was obtained as follows: the cells were painted using the Excel conditional formatting function. Then all heat maps were combined into one averaged heat map. On the basis of the average heat map, the transition boundaries were defined. Then lines coinciding with the largest diameters of elliptical

shading were drawn through the transition boundary reference points.

Temperature distribution graphs were created in cross sections, and the distance between the opposite cross sections of the graphs made it possible to determine the permissible sensor setting step.

V. Results and Discussions

A comparison of the test results (Fig. 9) shows a reduction in design strength between 1.1% and 7.3% over the entire curing period caused by environmental influences, such as temperature and humidity. However, at the end of 28 days the estimated strength has reached 33 MPa, which proves the compliance of the mixture with M350 grade B25. Moreover, the superposition of values showed a high degree of correlation equal to one (Fig. 10).

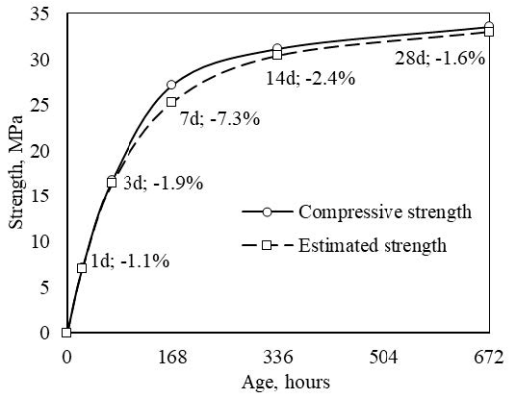

Fig. 9 Comparison of strength curves

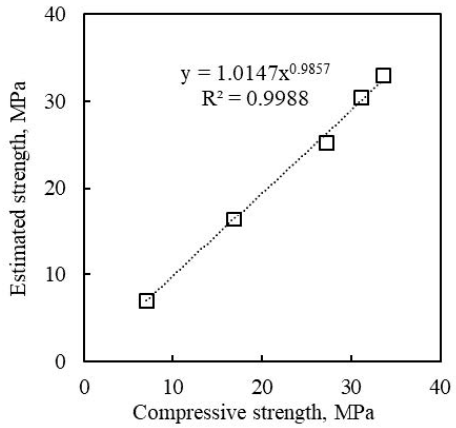

Fig. 10 Behavior and relationship of the compressive and estimated strengths

As mentioned earlier, the temperature inside the reinforced concrete slab was measured by sensors over a period of 28 days at 1-hour intervals. In this way, 672 temperature readings were collected. It can be seen from Fig. 11 that as the concrete cured, the temperature varied at different points on the slab, indicating that the concrete did not gain strength uniformly. This can be explained by the poor quality of the mixture or human error. On the second measurement day, the average internal temperature reached its peak. The highest temperature of 50 °C was recorded on the third sensor number 5. On the second day, sensor number 3 recorded a temperature of 47 °C. On average, the temperature peaks in other sensor locations range from 45 °C to 49 °C. Thus, for every hour during 28 days 672 heat maps were received. The heat maps for the most important ages of 3 days, 7 days and 28 days of concrete curing are shown in Figs. 11 (a), (b) and (c) respectively.

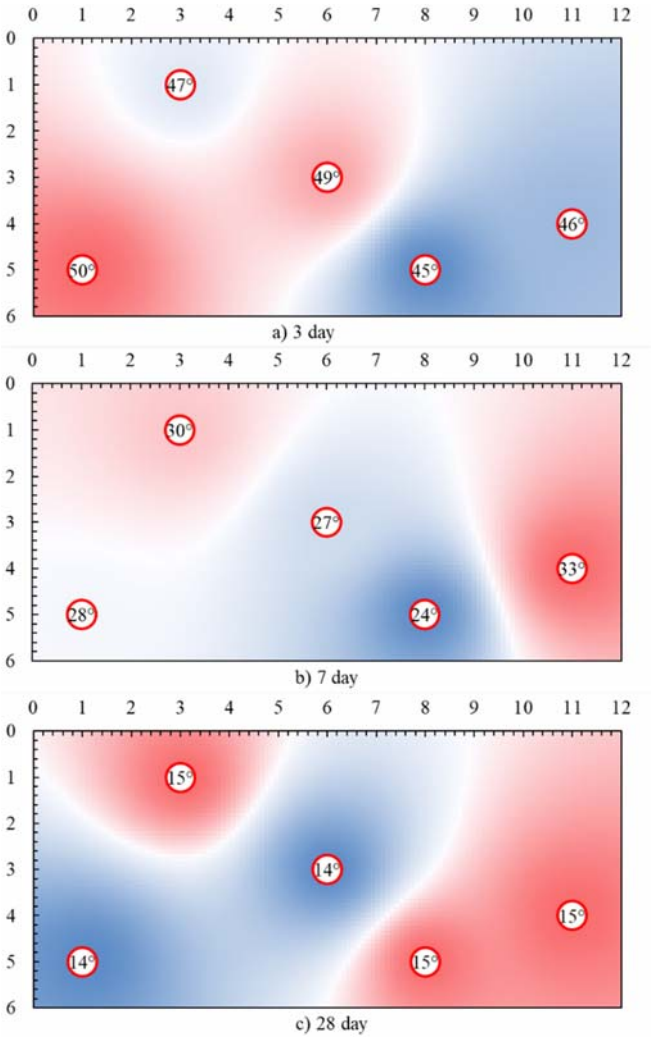

Fig. 11 Heat maps of temperature distribution

From Fig. 11, it is possible to understand the temperature change during 28 days of concrete curing. To demonstrate the temperature changes in the plane on the heat maps, three scaled colors were used: blue, white and red. Cells painted blue and red represent the lower and upper temperature values respectively. White indicates the transitional boundaries between the lower and upper temperature values.

An average heat map was created on the basis of numerous heat maps in order to obtain a general concept of optimal sensor placement (Fig. 12). Thus, according to the last operation of this study, diagrams of temperature distribution over the sections A-A, B-B and C-C passing through the control points were created. For sensors no. 2, 3 and 4, cross sections at 45°, 110°

and 0° to the horizontal axis respectively were selected and temperature distribution diagrams presented in Fig. 13 were created.

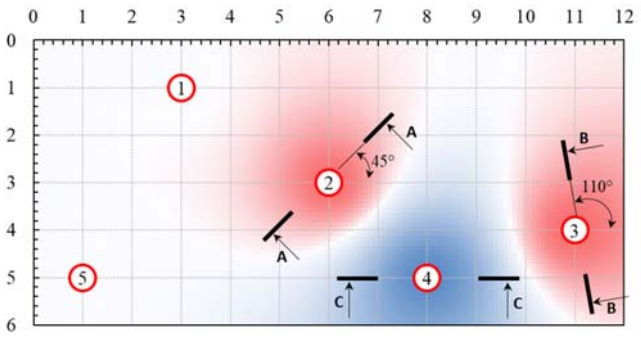

Fig. 12 Heat map of average temperature distribution

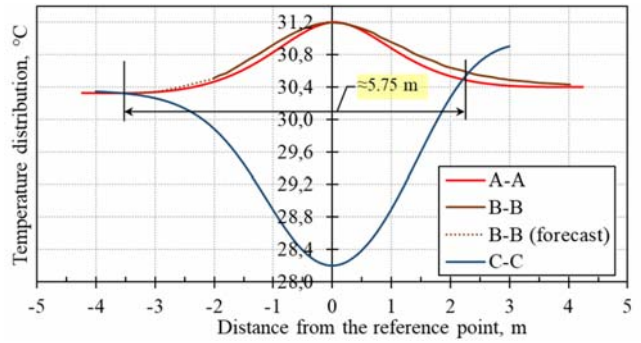

Fig. 13 Distribution of temperature at cross-sections

Based Fig. 13, it can be seen that temperatures in the cross-sections were in the range from 28.2 °C to 31.2 °C. The graphs (Fig. 13) have a parabolic shape with peaks in the vertical axis. High peaks are observed in reverse parabolic plots A-A and B-B, where the highest temperature values were determined (Fig. 12). Conversely, the lower peak is observed in chart C-C. Since the lower part of the cross-section B-B lies close to the boundary of the 2D plane, its temperature distribution graph has been extended (marked with a dashed line) to provide intersection with the C-C graph, which has a lower peak. When looking at the A-A and B-B graphs, one can notice that their transitional boundaries start at an average distance of 3.5 m from the reference points. In case of graph C-C, on one side (left) the transitional boundary starts at a distance of 4 m, and on the other side (right) - at a distance of 3 m from the anchor points. To get the total effect of all temperature distribution graphs, it is suggested to pay attention to the intersection of the graphs on both sides. Such intersections can create several new asymmetric shapes, depending on the number of taken sections. It is suggested to consider the distance between the closest opposite intersections of the temperature distribution graphs, represented by regular and reverse parabolic plots, as the maximum allowed step of maturity sensors settings. In addition, to facilitate the selection of intersections, it is proposed to consider an asymmetric form with the smallest area, which takes up more space inside compared to other asymmetric forms. In this study, a distance of 5.75 m was found between two opposite intersections of temperature distribution graphs based on the three cross-sections considered. Thus, the placement step of the maturity sensors should be smaller than this distance.

VI. Conclusions

To date, in Kazakhstan embedded wireless sensors to control the strength of concrete have not found wide application for a number of reasons, such as: relatively high cost; high labor intensiveness (associated with a sequential synchronization of smartphone with sensors); absence of standards regulating their applicability. In addition, previous studies have poorly covered the issue of the optimal placement of sensors in the concrete body, giving only logical suggestions.

The developed prototype of maturity sensor allows monitoring of the internal condition of the reinforced concrete structure, determining its strength, rather accurately. On the basis of the sensor readings, it is possible to make forecasts about the strength gain of the structure, thus achieving cost and time savings by timely removal of the formwork and loading the structure.

Tests on the prototype have confirmed its performance. The optimal sensor placement step in the concrete is set experimentally - no more than 5.75 m between sensors.

During the tests, no defects were detected, but the prototype can be further improved in the following parameters:

1) Reducing the size and shape of the case;
2) Use of a different data transfer protocol. By using Bluetooth to collect measurement data, the smartphone has access to no more than one device at a time. The same problem can be observed in foreign analogs. Narrowband IoT can eliminate this disadvantage;
3) Mobile application development;
4) Testing under different conditions (rain, snow).

Acknowledgement

This research has been funded by the Science Committee of the Ministry of Education and Science of the Republic of Kazakhstan (Grant No. AP08052033).

References

[1] Kibar H., Ozturk T. Determination of concrete quality with destructive and non-destructive methods // Comput. Concr. Techno-Press, 2015. Vol. 15, № 3. P. 473–484.
[2] Malek J., Kaouther M. Destructive and non-destructive testing of concrete structures // Jordan J. Civ. Eng. Jordan University of Science and Technology: Deanship of Research, 2014. Vol. 159, № 3269. P. 1–10.
[3] Putman B.J., Neptune A.I. Comparison of test specimen preparation techniques for pervious concrete pavements // Constr. Build. Mater. Elsevier, 2011. Vol. 25, № 8. P. 3480–3485.
[4] Thandavamoorthy T.S. Determination of concrete compressive strength: A novel approach // Pelagia Res. Libr. Adv. Appl. Sci. Res. 2015. Vol. 6, № 10. P. 88–96.
[5] Rehman S.K.U. et al. Nondestructive test methods for concrete bridges: A review // Constr. Build. Mater. Elsevier, 2016. Vol. 107. P. 58–86.
[6] Helal J., Sofi M., Mendis P. Non-destructive testing of concrete: A review of methods // Electron. J. Struct. Eng. 2015. Vol. 14, № 1. P. 97–105.
[7] Erdal H. et al. Prediction of concrete compressive strength using non-destructive test results // Comput. Concr. Techno-Press, 2018. Vol. 21, № 4. P. 407–417.
[8] Lim Y.Y. et al. Non-destructive concrete strength evaluation using smart

piezoelectric transducer—A comparative study // Smart Mater. Struct. IOP Publishing, 2016. Vol. 25, № 8. P. 85021.
[9] Hannan M.A., Hassan K., Jern K.P. A review on sensors and systems in structural health monitoring: Current issues and challenges // Smart Struct. Syst. Techno Press, 2018. Vol. 22, № 5. P. 509–525.
[10] Dutta S., Samui P., Kim D. Comparison of machine learning techniques to predict compressive strength of concrete // Comput. Concr. Techno-Press, 2018. Vol. 21, № 4. P. 463–470.
[11] Apostolopoulour M. et al. Prediction of compressive strength of mortars using artificial neural networks // Proceedings of the 1st international conference TMM_CH, transdisciplinary multispectral modelling and cooperation for the preservation of cultural heritage, Athens, Greece. 2018. P. 10–13.
[12] Gazder U. et al. Predicting compressive strength of bended cement concrete with ANNs // Comput. Concr. Techno-Press, 2017. Vol. 20, № 6. P. 627–634.
[13] Fick G.J. et al. Field reference manual for quality concrete pavements. 2012.
[14] Utepov Y.B. et al. Maturity sensors placement based on the temperature transitional boundaries. // Mag. Civ. Eng. 2019. Vol. 90, № 6. P. 93–103.
[15] Taheri S. A review on five key sensors for monitoring of concrete structures // Constr. Build. Mater. Elsevier, 2019. Vol. 204. P. 492–509.
[16] Ge Z., Wang K. Modified heat of hydration and strength models for concrete containing fly ash and slag // Comput. Concr. Techno-Press, 2009. Vol. 6, № 1. P. 19–40.
[17] Zemajtis J.Z. Role of concrete curing // Portl. Cem. Assoc. Skokie. 2014.
[18] Anwar Hossain K.M. Influence of extreme curing conditions on compressive strength and pulse velocity of lightweight pumice concrete // Comput. Concr. Techno-Press, 2009. Vol. 6, № 6. P. 437–450.
[19] Chen H.-J., Yang T.-Y., Tang C.-W. Strength and durability of concrete in hot spring environments // Comput. Concr. 2009. Vol. 6, № 4. P. 269–280.
[20] Zhang B., Cullen M., Kilpatrick T. Spalling of heated high performance concrete due to thermal and hygric gradients // Adv. Concr. Constr. 2016. Vol. 4, № 1. P. 1–14.
[21] Farzampour A. Temperature and humidity effects on behavior of grouts // Adv. Concr. Constr. 2017. Vol. 5, № 6. P. 659.
[22] Kessler F., Battersby S. Working with Map Projections: A Guide to Their Selection. CRC Press, 2019. 65 p.
[23] Nath P., Hu Z., Mahadevan S. Sensor placement for calibration of spatially varying model parameters // J. Comput. Phys. Elsevier, 2017. Vol. 343. P. 150–169.
[24] Weighting I.D. Interpolation // GISGeography URL https//gisgeography.com/inverse-distance-weighting-idw-interpolation/(датаобращения 27.06. 2019).

Ye. B. Utepov was born in Abai village of South Kazakhstan region in 1990. He received his Ph.D degree in civil engineering at the L.N. Gumilyov Eurasian National University, Nur-Sultan, Kazakhstan in 2014.

His work experience is as follows: Engineer-estimator at the DK-Santekh LLP, Design-engineer at the Zangar-Orda LLP, Foreman at the KGS-Astana LLP, R&D Expert at the JSC BI Group, Project team leader at the Niistromprojekt LLP. His current position is a Head of R&D at the CSI Research&Lab LLP, Nur-Sultan, Kazakhstan and an Acting Professor at the L.N. Gumilyov Eurasian National University, Nur-Sultan, Kazakhstan. His research interests comprise building materials, geotechnics, GIS and sensor technologies.

Dr., Assoc. Prof. Ye. B. Utepov is a member of the International Society for Soil Mechanics and Geotechnical Engineering (ISSMGE) since 2011.

A.S. Tulebekova was born in Karaganda, Kazakhstan in 1985. She received her Ph.D degree in civil engineering at the L.N. Gumilyov Eurasian National University, Nur-Sultan, Kazakhstan in 2012.

Her work experience is as follows: Senior Researcher at the KGS-Astana LLP, Teacher at the Technical College. Her current position is Senior Researcher at the CSI Research&Lab LLP, Nur-Sultan, Kazakhstan and an Acting Professor at the L.N. Gumilyov Eurasian National University, Nur-Sultan, Kazakhstan. Her research interests comprise geotechnics, standardization in construction, sensor technologies.

Dr., Assoc. Prof. A. S. Tulebekova is a member of International Society for Soil Mechanics and Geotechnical Engineering (ISSMGE) since 2012, General Secretary of Kazakhstan Geosynthetics Society since 2015.

A. B. Kazkeyev was born in Semey, East Kazakhstan in 1996. He received his M.Sc. degree in civil engineering at the L.N. Gumilyov Eurasian National University, Nur-Sultan, Kazakhstan in 2020.

His current position is a Junior Researcher at the CSI Research&Lab LLP, Nur-Sultan, Kazakhstan. His research interests comprise building materials, sensor technologies and simulation modeling.